

## Emissivities of $\gamma$ & $e^\pm$ and FERMI-PAMELA-AMS02

T. SHIBATA<sup>1</sup>, Y. OHIRA<sup>1</sup>, K. KOHRI<sup>2</sup>, R. YAMAZAKI<sup>1</sup>

<sup>1</sup> Department of Physics and Mathematics, Aoyama-Gakuin University, Kanagawa, 229-8558, Japan

<sup>2</sup> KEK Theory Center and the Graduate University for Advanced Studies (Sokendai), 1-1 Oho, Tsukuba 305-0801, Japan

shibata@phys.aoyama.ac.jp

**Abstract:** Recently the observations of high energy cosmic-rays (CRs) in space are developed remarkably with higher statistics and unprecedented precision, e.g. FERMI for  $\gamma$ 's and PAMELA-AMS02 for  $e^\pm$ 's as well as charged hadrons with antiparticles. They remove greatly the uncertainties in modeling for the high energy galactic phenomena, particularly today in the interpretation for the dramatical increase of positron fraction, far beyond the standard model for the production of positron and subsequent propagation to the Earth. In this paper, we give the production cross-section of  $\gamma$  and secondary  $e^\pm$  induced by p-p collision, which reproduces nicely the machine data, even with LHC, covering very wide energy ranges, 1 GeV-20 PeV. With these cross-sections, we present the intensity of diffuse  $\gamma$ -rays ( $D\gamma$ 's), and the positron fraction with use of the *same* numerical values in galactic parameters, each compared with FERMI, and PAMELA-AMS02 respectively.

**Keywords:** gamma-ray, positron, cross-section

### 1 Introduction

In Paper I [1], we present the production cross-section of  $\gamma$ 's,  $\sigma_{pp \rightarrow \gamma}$ , in p-p collision, applicable even for LHC forward experiment (LHCf). We apply it for the cross-section of  $e^\pm$ ,  $\sigma_{pp \rightarrow e^\pm}$ , produced via  $\pi^\pm - \mu^\pm - e^\pm$  decay. We find that  $\sigma_{pp \rightarrow \gamma}$  and  $\sigma_{pp \rightarrow e^\pm}$  are equivalent in the sense that they are kinematically linked with each other without back to the parent pion, either  $\pi^0$  or  $\pi^\pm$ , but different only in the mass,  $m_\gamma$  and  $m_{e^\pm}$ . So once we have  $\sigma_{pp \rightarrow \gamma}$ , we obtain immediately  $\sigma_{pp \rightarrow e^\pm}$ , reliable enough up to TeV-PeV region.

With use of  $\sigma_{pp \rightarrow \gamma}$  and  $\sigma_{pp \rightarrow e^\pm}$  well confirmed by the machine data, we present firstly the intensity of  $D\gamma$ 's, and secondly so called the positron fraction,  $e^+/[e^+ + e^-]$ , each compared with FERMI, and PAMELA-AMS02 respectively in the following sections.

### 2 Production cross-sections of $\gamma$ & $e^\pm$ in p-p collision

In this section we briefly give only  $\sigma_{pp \rightarrow \gamma}$  because of limited space, see references [1, 2] for the detail of  $\sigma_{pp \rightarrow \gamma}$  and  $\sigma_{pp \rightarrow e^\pm}$ , taking the contribution of isobaric resonance into account.

We present explicitly the semi-empirical energy spectrum of  $\gamma$ -rays below,

$$\frac{dN_\gamma}{dE_\gamma} = \frac{\sigma_{pp \rightarrow \gamma}(E_0, E_\gamma)}{\sigma_{pp}(E_0)} = \bar{N}_\gamma \varphi(E_0, E_\gamma);$$

$$\frac{\varphi(E_0, E_\gamma)}{\beta_c^2 \Theta_c} = \frac{1}{M_p} \int_{\omega_-}^{\omega_+} \frac{(1 - x_\gamma \Gamma_\theta)^4}{\Gamma_\theta + \zeta \tau_\theta} e^{-\tau_\theta x_\gamma} d\omega,$$

with  $\zeta = 0.02$ ,  $\omega = \cos \theta$ , and

$$x_\gamma = \frac{E_\gamma}{E_0} \left[ 1 + \frac{m_{\pi^0}^2}{4E_\gamma^2} \right]; \quad \omega_\pm = \beta_c^{-1} - \beta_c^{\pm 1} e^{\pm \eta_0^* - \eta_\gamma^*},$$

$$\eta_0^* = \ln(2\beta_c \gamma_c M_p / m_{\pi^0}); \quad \eta_\gamma^* = \ln(2\beta_c \gamma_c E_\gamma / m_{\pi^0}),$$

$$\tau_\theta = (E_0/p_0) \sin \theta; \quad \Gamma_\theta = (E_0/M_p)(1 - \beta_c \cos \theta),$$

where  $E_0$  is the kinetic energy of projectile proton in the laboratory system (LS),  $\sigma_{pp}(E_0)$  the total inelastic cross-section in p-p collision,  $\bar{N}_\gamma$  the *effective*  $\gamma$ -ray multiplicity, which is determined by the machine data, and  $\beta_c$  ( $\gamma_c$ ) is the velocity (Lorentz factor) of center of mass system (CMS) with respect to LS,  $\Theta_c$  the normalization constant,  $M_p$  the mass of proton,  $p_0$  approximately corresponding to the average transverse momentum of  $\gamma$ -rays, see [1, 2] for more detail.

In Fig. 1, We demonstrate an example of the comparison between our parametrization in  $\sigma_{pp \rightarrow \gamma}$  and the most recent LHCf data [3] at  $\sqrt{s} = 900$  GeV, corresponding to approximately 400 TeV in laboratory energy.

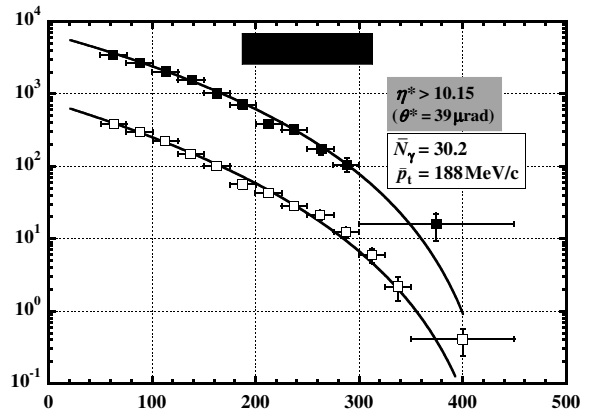


**Fig. 1:** Comparison between our parametrization for the production cross-section of  $\gamma$  and those observed by the most recent LHCf experiment at  $\sqrt{s} = 900$  GeV.

### 3 Normalization of the proton and the primary-electron intensities

In order to calculate the intensity of the  $D\gamma$ 's and the positron fraction, we need both intensities of the proton and the primary electron spectra. So we use the absolute ones at the normalization energy both with  $\bar{E}_n = 100$  GeV nowadays available in the solar system (SS), which are free from the modulation effect as well as from the observational uncertainty in both statistics and the experimental precision, while scatters considerably among authors in the higher energy region  $\gtrsim 1$  TeV.

Let us present the explicit value of the proton density at the SS,  $\bar{N}_{n,p}^\odot \equiv N_p(\vec{r}_\odot, \bar{E}_n)$  with  $(E_0, \vec{r}) = (\bar{E}_n, \vec{r}_\odot)$ ,

$$c\bar{N}_{n,p}^\odot = 6.22 \times 10^{-1} \text{ (m}^{-2}\text{s}^{-1}\text{GeV}^{-1}\text{)},$$

based on the current proton intensity at  $E_0 = 100$  GeV,

$$E_0^{2.5} \frac{dI_p^\odot}{dE_0} = 4.95 \times 10^3 \text{ (m}^{-2}\text{s}^{-1}\text{sr}^{-1}\text{GeV}^{1.5}\text{)},$$

which is consistent with the past (for instance, Derbina et al. [4]) and the most recent PAMELA data [5].

Additionally we need the absolute electron density at the normalization energy  $\bar{E}_n = 100$  GeV in the following

$$c\bar{N}_{n,e}^\odot = 1.86 \times 10^{-3} \text{ (m}^{-2}\text{s}^{-1}\text{GeV}^{-1}\text{)},$$

based on the current electron intensity at  $E_e = 100$  GeV mainly focussing on FERMI [6], PAMELA [7], and the ECC data most recently revised by Kobayashi et al. [8],

$$E_e^3 \frac{dI_e^\odot}{dE_e} = 1.49 \times 10^2 \text{ (m}^{-2}\text{s}^{-1}\text{sr}^{-1}\text{GeV}^2\text{)},$$

which is important to calculate the positron fraction to all electrons,  $e^+/(e^+ + e^-)$ , as seen later.

Here we have to separate  $c\bar{N}_{n,e}^\odot$  into two components, one from (1) the *surviving* primary electrons, and the other from (2) the secondary ones induced by the charged pions via  $\pi^\pm$ - $\mu^\pm$ - $e^\pm$  decays,

$$c\bar{N}_{n,e}^\odot = c\bar{N}_{n,1}^\odot + c\bar{N}_{n,2}^{\odot\pm},$$

while the contribution of the second components is of as large as 10% around 100 GeV.

### 4 Intensity of $D\gamma$ 's and FERMI data

The  $D\gamma$ 's come from two origins, one from the hadronic collisions between CRs (mainly proton) and the ISM gas (mainly hydrogen with approximately 10% helium in number), and the other from the electromagnetic interactions between the primary electrons and ISRF & ISM gas in the forms of inverse Compton scattering (IC) & the bremsstrahlung (EB) respectively.

Explicit procedure in calculating the  $D\gamma$ 's intensity is performed by one of the authors (T. S.) [9], and the revised one is recently presented by the present authors with use of the more reliable cross-section in  $\sigma_{pp \rightarrow \gamma}$  [2], which is valid even for LHC energy region. In these calculations we take the nuclei effect into account by introducing the nuclear enhancement factor with  $\varepsilon_H = 1.53$  [10].

In Fig. 2, we present the energy spectrum of  $D\gamma$ 's coming from the sky view rather close to the galactic plane,

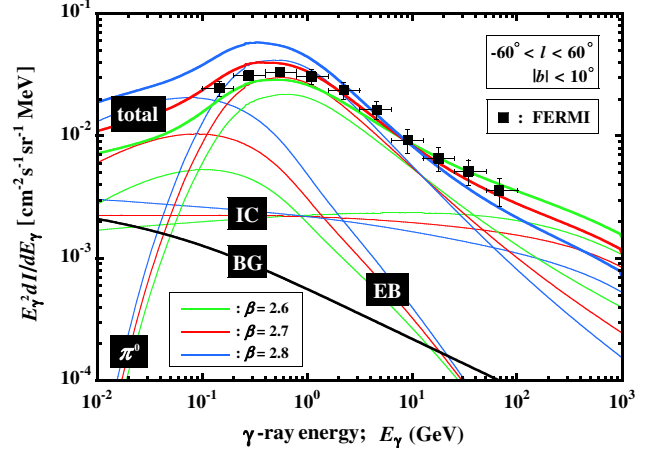


**Fig. 2:** Differential energy spectra of  $D\gamma$ 's averaged over the field of view with  $-60^\circ < l < 60^\circ$  and  $|b| < 10^\circ$  obtained by FERMI [12], where we assume three spectral indices for proton spectrum with  $beta = 2.6$  (green),  $2.7$  (red), and  $2.8$  (blue).

$|b| < 10^\circ$ , with the galactic longitude from  $-60^\circ$  to  $+60^\circ$ , where BG (heavy solid curve) denotes the background  $\gamma$ 's obtained by FERMI [11], coming from extragalactic sources, unidentified ones, and others (darkmatter?).

Here and in the following, we always assume three indices of the *source* spectrum,  $\gamma = 2.27, 2.37, \text{ and } 2.47$ , corresponding to those of the spectrum at the SS,  $\beta (= \gamma + \alpha) = 2.6, 2.7, \text{ and } 2.8$  with  $\alpha = \frac{1}{3}$  for Kolmogorov-type turbulence. Note that the normalization for the proton energy spectrum at 100 GeV is common irrespective of the choice of  $\beta$ . So one may find that three curves (green, red, blue) in Fig. 2 coincide around  $E_\gamma \approx 10$  GeV, corresponding to approximately 100 GeV in the parent proton energy.

On the other hand, in Fig. 3a-c, we present those distant from the galactic plane for different sky views (Abdo et al. [13]; see also supplemental material on line at <http://link.aps.org/supplemental/10.1103/PhysRevLett.104.101101>), averaged over independent galactic latitude ranges covering (a) low, (b) mid, and (c) high galactic latitudes, each with  $10^\circ < |b| < 20^\circ$ ,  $20^\circ < |b| < 60^\circ$ , and  $60^\circ < |b| < 90^\circ$ , respectively.

One finds that the present calculations reproduce excellently the FERMI  $D\gamma$ 's data for  $|b| < 60^\circ$  (Figs. 2 and 3a, 3b), both in *shape* and the *absolute value*. However, as was pointed out already in Paper II [9], the  $D\gamma$ 's intensity coming from the high latitude in Fig. 3c with  $|b| > 60^\circ$  is as large as the twice of expected, much beyond the uncertainty in numerical calculations,  $\sim 30\%$  even at worst.

So looking carefully once again Fig. 3b with the mid latitude  $20^\circ < |b| < 60^\circ$ , it is of approximately 20% higher than expected, albeit possibly within the uncertainty in the numerical calculation. Nevertheless we are very concerned about the systematic enhancement of  $D\gamma$ 's coming from somewhere around the galactic pole direction.

### 5 Positron fraction and PAMELA-AMS02 data

Now, in Fig. 4, we present the current experimental data with the hot AMS02 data (Aguilar et al. [14]) on the positron

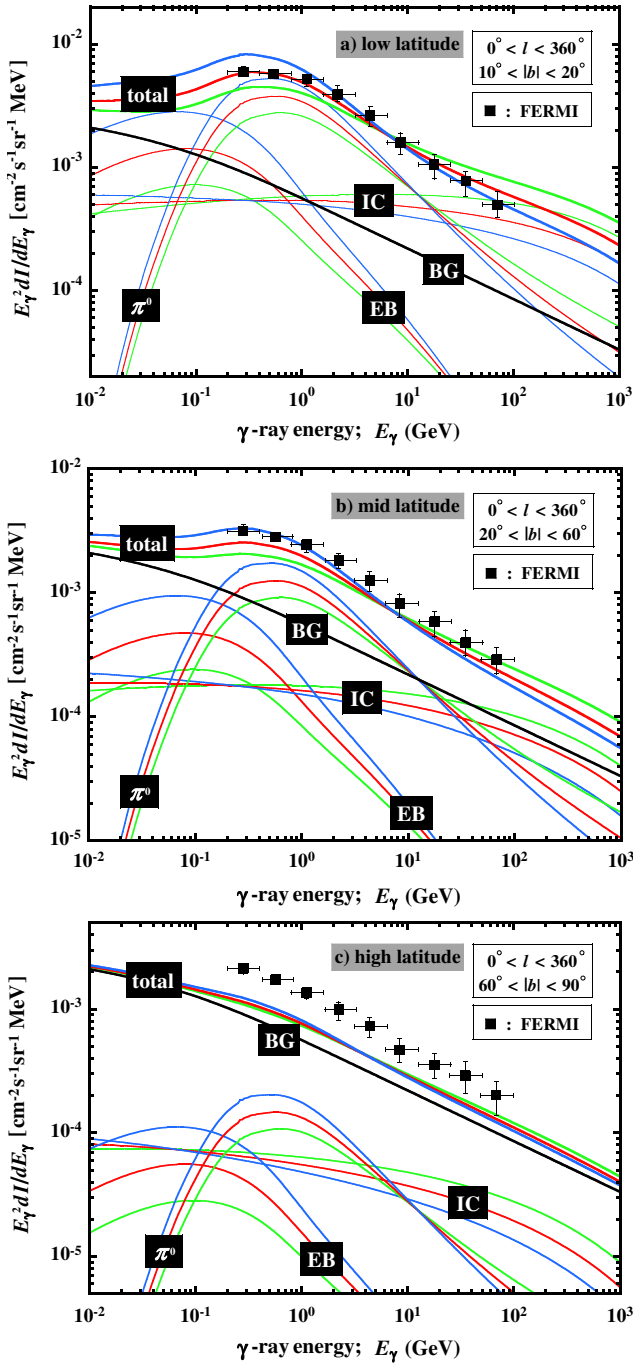


**Fig. 3:** Same as Figure 2, but those averaged over three different ranges in the galactic latitude: (a) low latitude with  $10^\circ < |b| < 20^\circ$ , (b) mid latitude with  $20^\circ < |b| < 60^\circ$ , and (c) high latitude with  $60^\circ < |b| < 90^\circ$ .

fraction to all electrons,  $e^+/(e^+ + e^-)$ , together with our calculations for  $\beta =$  (a) 2.6, (b) 2.7, and (c) 2.8 with the nuclear enhancement factor  $\varepsilon_H = 1.53$ , where we present curves with four modulation parameters,  $\Phi = 200, 400, 600,$  and  $800$  MV, using the force field approximation (Gleeson and Axford [15]).

While they are in good agreement with each other for lower energy region,  $E_e \lesssim 3$  GeV, one may claim that PAMELA-AMS02 data and our curves deviate significantly from AMS01, HEAT, etc. at low energies  $\lesssim 10$  GeV. The

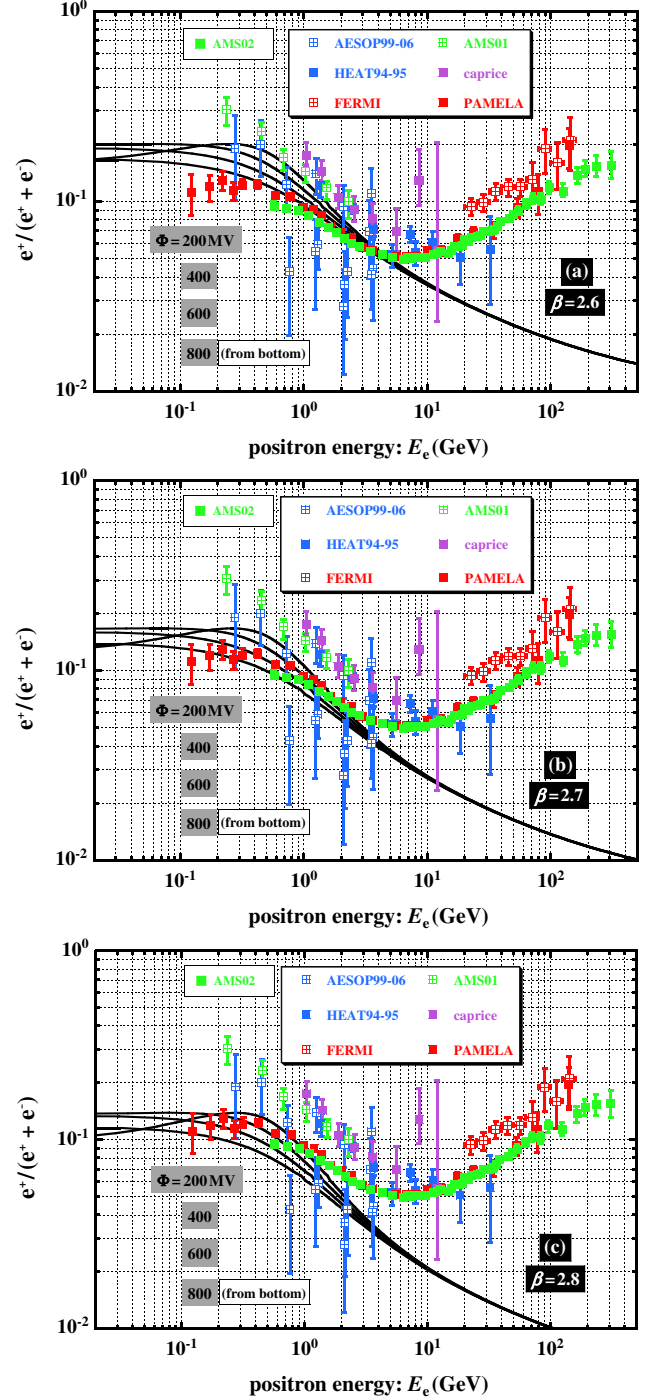


**Fig. 4:** Positron fraction currently available, together with our calculations, where we assume three spectral indices, (a)  $\beta = 2.6$ , (b)  $\beta = 2.7$ , and (c)  $\beta = 2.8$ .

deviation is understood in the framework of the charge-sign-dependent solar modulation, and its effect is well studied with the drift model (Moskalenko et al. [16]).

According to Beischer et al. [17], they find the PAMELA data is consistent enough with the pre-PAMELA ones such as AMS01 (Alcaraz et al. [18]; Aguilar et al. [19]), HEAT (Beatty et al. [20]), CAPRICE (Boezio et al. [21]), and TS93 (Golden et al. [22]), using the GALPLOP code with the charge-sign-modulation, while including great uncertainties in the modeling as yet.

Fortunately they show explicitly the correlation between

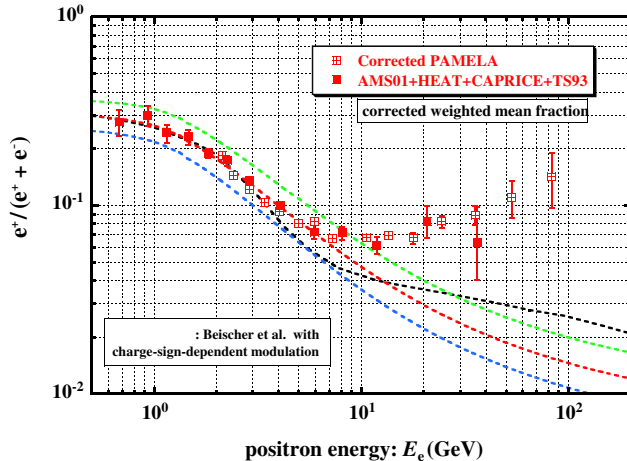


**Fig. 5:** Positron fraction after the correction for the charge-sign-dependent solar modulation effect according to the GALPROP code based on the drift model, both for the data and the calculations.

the positron fraction  $e^+/(e^+ + e^-)$  and the positron energy  $E_e$  every data points both with and without the charge-sign-modulation based on the GALPROP code. Applying the correlation between them thus obtained for the uncorrected fractions with  $\Phi = 400$  MV in Fig. 4, we present the corrected curves (dotted colors) in Fig. 5, together with the corrected data, where four data, AMS01, HEAT, ACAPRICE, and TS93, are all combined with some statistical weights [17]. We find good agreement each other in the low energy region, while we should keep in mind that the correction is not model-independent one, including much uncertainties in modulation modeling such as heliospheric magnetic field, the tilt of the current sheet, and so forth.

## 6 Summary and conclusion

With use of the refined production cross-sections for  $\gamma$  and  $e^\pm$  in p-p collisions, we present the intensity of  $D\gamma$ 's and the positron fraction at the SS, using the *same* numerical values in galactic parameters. We compared our numerical curves thus obtained with FERMI [12] for the former, and mainly PAMELA [23] & AMS02 [14] for the latter respectively.

As pointed out by previous other works from the early period (for instance HEAT, DuVernois et al. [20]) to nowadays (PAMELA and AMS02), we find again the significant rise in positron fraction compared to the numerical calculations based on the standard model for the production of  $e^\pm$  and subsequent propagation to the Earth.

While it is indeed in an outstanding question today for the undoubted rise in positron fraction with energy  $E_e \gtrsim 10$  GeV, either due to the cosmological origin such as the darkmatter or from the astronomical one such as for instance nearby pulsar, we are concerned also about the excess of  $D\gamma$ 's coming from the galactic pole direction as observed by FERMI (see Figure 3c), which is already remarked by, for instance, Keshet et al. [24], pointing out a possibility of a signature of very large electron-halo far distant from the galactic plane. We will study the relation between the excess of the  $D\gamma$  intensity in GeV region and that of the positron fraction in  $E_e \gtrsim 5$  GeV elsewhere.

Another point we are concerned about is the normalization in proton spectrum. Namely in order to estimate the positron fraction, we need to normalize both proton and electron intensities at 100 GeV as presented in Section 3, which are reliable enough even today around there, as the statistics is rather rich with small scatterings among authors.

However, we should not forget that the spectral shape, i.e., the index  $\beta$  in proton and electron spectra is quite essential in both lower and the higher energy regions, particularly in the latter. If we assume another spectral shape (or energy-dependent one) in the primary components either with softer or harder ones, we must get another numerical results on the positron fraction. For instance, recent data on the proton and the helium spectra by ATIC (Wefel et al. [19]), CREAM (Ahn et al. [20]) and PAMELA (Adriani et al. [5]) report all the drastic hard spectrum already in the energy region  $\gtrsim 100$ -200 GeV, which must result in the hard spectrum of positrons in the higher energy region, leading to the drastic increase in the positron fraction.

In the near future, we will study the origin of the anomaly in positron fraction from the theoretical point of view, based on the present results as well as the full data with the *absolute* intensities for various elements such as  $e^\pm$ ,  $p$ , and  $\bar{p}$  by AMS02.

## References

- [1] Sato, H., Shibata, T., and Yamazaki, R. 2012, *Astropart. Phys.* 36, 83 (Paper I)
- [2] Shibata, T., Ohira, Y., Kohri, K., and Yamazaki, R. arXiv:1304.0879v1 [astro-ph.HE] 3 Apr 2013
- [3] Adriani, O., et al. 2012, arXiv:1207.7183v1 [hep-ex] 31 Jul 2012
- [4] Derbina, V. A., et al. 2005, *ApJ*, 628, L41
- [5] Adriani, O., et al. 2011, *Phys. Lett. B*, 703, 128
- [6] Ackermann, M. et al. 2010, *Phys. Rev. D*, 82, 092004
- [7] Adriani, O., et al. 2009, *Nature* 458, 607 (2009)
- [8] Kobayashi, T., et al. 2012, *ApJ*, 760, 146
- [9] Shibata, T. et al. 2011, *ApJ*, 727, 38
- [10] Shibata, T. et al., 2007, *Astropart. Phys.*, 27, 411
- [11] Abdo, A. A. et al. 2010a, *ApJ*, 720, 435 (2010)
- [12] Ackermann, M. et al. 2010, *Phys. Rev. D*, 82, 092004
- [13] Abdo, A. A. et al. 2010b, *Phys. Rev. Lett.*, 104, 101101 (2010)
- [14] Aguilar, M., et al. (AMS Collaboration) 2013, *Phys. Rev. Lett.* 110, 141102
- [15] Gleeson, I.J., and Axford, W.I. 1968, *ApJ*, 154, 1011
- [16] Moskalenko, I.V. et al. *ApJ*, 565, 280 (2002)
- [17] Beischer, B. et al. 2009, *New J. Phys.* 11, 105021
- [18] Alcaraz, J., et al. 2000, *Phys. Lett. B* 484, 10
- [19] Aguilar, M., et al. 2007, *Phys. Lett. B* 646, 145
- [20] Beatty, J.J. et al. 2004, *Phys. Rev. Lett.* 93, 241102
- [21] Boezio, M. et al. 2000, *ApJ*, 532, 653
- [22] Golden, R. L., et al. 1996, *ApJ*, 457, L103
- [23] Picozza, P., Proc. of the 4th International Conference on Particle and Fundamental Physics in Space, Geneva, 5-7 Nov. 2012
- [24] Keshet, U. et al. 2004, *J. Cosmol. Astropart. Phys.*, JCAP04(2004)006
- [25] Wefel, J. et al. 2008, Proc. 31th Int. Cosmic Ray Conf., (Lodz), 2, 31
- [26] Ahn, H.S. et al. 2010, *ApJ*, 714, L89